This is a “preproof” accepted article for *Animal Nutriomics*.

This version may be subject to change during the production process.

10.1017/anr.2024.26

Title:

Betaine increases intramuscular fat deposition by promoting the cell cycle via a manner involving NADPH/FTO/m^{6}A signaling

Authors:

Jiaqi Liu[a,b,c,d#], Tongyudan Yang[a,b,c,d#], Yuxi Liu[a,b,c,d], Youhua Liu[a,b,c,d], Chaoqun Huang[a,b,c,d], Xinxia Wang[a,b,c,d]*

Affiliations:

[a] College of Animal Sciences, Zhejiang University, Hangzhou, 310058, China

[b] Key Laboratory of Molecular Animal Nutrition (Zhejiang University), Ministry of Education, Hangzhou, 3100058, China

[c] Key Laboratory of Animal Nutrition and Feed Science (Eastern of China), Ministry of Agriculture and Rural Affairs, Hangzhou 310058, China

[d] Key Laboratory of Animal Feed and Nutrition of Zhejiang Province, Hangzhou 310058, China

[#]Equal contributors: Jiaqi Liu, Tongyudan Yang

[*]Corresponding author: Xinxia Wang

E-mail: xinxiawang@zju.edu.cn

Tel: +86 13067753599

Abstract

Intramuscular fat (IMF) content is a critical indicator of meat quality in livestock production and possesses significant medical relevance for human health. Betaine, a naturally occurring alkaloid compound, holds considerable potential as a nutritional approach for regulating intramuscular adipogenesis, while its exact efficacy and underlying mechanisms still remain subjects of ongoing debate and investigation. Here, we clarified the enhancing effect of betaine on IMF deposition using porcine, murine, and cellular models. Mechanistically, betaine supplementation leads to a significant increase in nicotinamide adenine dinucleotide phosphate (NADPH) concentration in the liver, serum, and skeletal muscle. Elevated levels of NADPH upregulate the expression of fat mass and obesity-associated (FTO), a well-established N^6-methyladenosine (m^6A) demethylase, to diminish m^6A modification in skeletal muscle and intramuscular fat deposition. This process effectively promotes the mitotic clonal expansion (MCE) and subsequently intramuscular adipogenesis. In summary, our findings expand current understanding of the regulatory role of betaine in IMF deposition and sheds light on the molecular mechanisms underlying its modulation, which is conducive to producing high-quality and healthful pork.

Keywords

betaine, IMF, meat quality, NADPH, m^6A modification, MCE

1. Introduction

Intramuscular fat (IMF) refers to the adipose tissue situated between skeletal muscle fibers [1]. Since its positive influence on determining meat nutritional value, flavor, and juiciness [2,3], IMF content is commonly regarded as an important economic characteristic in livestock production [4]. Growing interest has been sparked in developing effective strategies to promote IMF deposition and subsequently elevate meat quality in animal husbandry. On the contrary, in human, excessive lipid accumulation within skeletal muscle is strongly associated with conditions such as obesity, insulin resistance, type 2 diabetes mellitus, and various metabolic diseases [5-7]. Therefore, comprehending the molecular underpinnings governing lipid metabolism and adipogenesis in skeletal muscle is of great economic and medical value, and may yield critical insights for enhancing meat quality or ameliorating metabolic dysregulation.

Dietary interventions are being explored to be an alternative to conventional breeding strategies

https://doi.org/10.1017/anr.2024.26 Published online by Cambridge University Press

for modulating IMF deposition recently. *N, N, N*-trimethylglycine, or normally named betaine, a neutral zwitterionic compound widely abundant in plants, animals, and microorganisms [8,9], holds considerable promise as a regulator for various physiological activities [8-14]. Several animal model-based studies have reported its potential in affecting IMF content [15-17]. However, the role of betaine in this context is still controversial [15,18], and the precise mechanisms by which betaine operates necessitate further investigation as well.

N^6-methyladenosine (m^6A), the most abundant mRNA modification in eukaryotes, exhibits rapid responsiveness in fine-tuning mRNA metabolism, including mRNA splicing, export, localization, translation, and stability [19,20]. Our previous research has characterized a distinct variation in the m^6A methylomes between high and low IMF content *longissimus dorsi* muscle samples [21], implying the involvement of m^6A modification in IMF deposition. What's more, it's well reported that betaine works as a methyl donor in the methionine cycle, participating in one-carbon metabolism to enhance the formation of S-adenosylmethionine [22]. These factors enable us to raise the conjecture of whether epigenetic modification regulation could be one of the mechanisms by which betaine alters IMF deposition.

Here, we aimed to provide a valuable resource from an epigenetics perspective to demonstrate that betaine could be a promising candidate for incorporation into dietary supplements to promote intramuscular adipogenesis, permitting us to better understand how to improve pork quality and offering a potential target for the therapy of metabolic diseases.

2. Materials and methods

2.1. Animal ethic statement

All animal experimental procedures were approved by the Committee on Animal Care and Use and the Committee on the Ethics of Animal Experiments of Zhejiang University (ZJU20240254) and were strictly carried out in accordance with the applicable regulations for animal experiments throughout the entire experimental period.

2.2. Animals study

(1) Duroc × Landrace × Yorkshire (DLY) crossed finishing pigs with an average body weight of 90.12 ± 2.20 kg were randomly divided into control group (CTL) and betaine group (BET) with three replicates per group (nine pigs per replicate). Pigs in the CTL were fed a basal diet, while

https://doi.org/10.1017/anr.2024.26 Published online by Cambridge University Press

those in the BET were fed a basal diet supplemented with 2500mg/kg betaine [23,24], with ad libitum access to food and water. The entire experimental period lasted for 45 days (5 days pre-feeding period and 40 days formal test period). We recorded the initial weight, final weight, and daily feed intake to calculate the average daily gain and average daily feed intake. At the end of the feeding, 6 pigs (close to the average body weight) from each group were selected and slaughtered after fasting for 12h. Within 20 min of slaughter, about 100 g samples of *longissimus thoracis* were obtained from the 3rd to 11th ribs on the right-side carcass rapidly, frozen in liquid nitrogen immediately, and subsequently stored at −80 °C for further assay.

Table 1 Ingredients and nutrient levels of experimental diets (%, air-dry basis).

Item	**Diet**	
	Control group	**Betaine group**
Ingredients		
Corn	47.70	47.70
Rice	5.00	5.00
Barley	15.00	15.00
Rice bran	8.00	8.00
Rice bran meal	8.00	8.00
Soybean meal	10.00	10.00
Soybean oil	2.30	2.30
Premix[1]	4.00	4.00
Total	100.00	100.00
Betaine, mg/kg	/	2500
Nutrition levels		
Digestible energy, MJ/kg	14.22	14.16
Crude protein	12.17	12.36
Crude fat	5.53	5.79
Crude ash	5.38	5.63
Calcium	0.58	0.59
Available phosphorus	0.32	0.33
Lysine	0.27	0.28
Methionine	0.60	0.59
Threonine	0.63	0.59
Tryptophan	0.17	0.16

https://doi.org/10.1017/anr.2024.26 Published online by Cambridge University Press

[1]Provided the following per kilogram of complete diet: vitamin A, 6,400 IU; vitamin B_1, 0.6 mg; vitamin B_2, 10.4 mg; vitamin D_3, 2,200 IU; vitamin E, 10 mg; vitamin K_3, 2 mg; biotin, 0.15 mg; D-pantothenic acid, 6.4 mg; nicotinic acid, 10 mg; Cu (as copper sulfate), 18 mg; Fe (as ferrous sulfate), 140 mg; Mn (as manganese sulfate), 36 mg; Zn (as zinc sulfate), 72 mg; I (as potassium iodide), 0.06 mg; Se (as sodium selenite), 0.44 mg.

(2) Six-week-old wild-type male C57BL/6J mice (*n*=12) were purchased from the Shanghai Model Organisms Center, Inc. (Shanghai, China). They were housed (no more than four individuals per cage) in a pathogen-free animal facility under a 12-hour light/dark cycle, 22 ± 1℃ room temperature, and 55 ± 5% humidity with unrestricted access to food and tap water. Following a one-week acclimatization period, mice were randomly allocated into two groups: standard laboratory chow diet (NCD, Jiangsu Xietong, XTCON50J) and NCD administered with a 2% (w/v) beet alkaline solution (Bet, Sigma-Aldrich, B2629) [25-27]. On the 42nd day, mice were injected with glycerin into skeletal muscle to induce fat infiltration [28,29], and subsequently sacrificed for sampling 14 days later. Tissues were dissected, weighed, and either soaked in formalin for later morphological analysis or immediately snap-frozen in liquid nitrogen for further analysis.

2.3. Primary mouse cell isolation

Mouse primary hepatocytes were isolated from 8-week-old male C57BL/6J mice following two-step-perfusion method as described previously [30]. The mice's abdominal cavity was opened under a painless anesthesia condition. Subsequently, in situ liver perfusion was conducted using HBSS without Ca^{2+} and Mg^{2+} (Gibco™, C14175500BT) containing 25 mM HEPES (Sigma-Aldrich, H6903) and 0.5 mM EDTA (Gibco™, R1021), followed by the digestion of liver using HBSS with Ca^{2+} and Mg^{2+} (Biological Industries, 02-015-1ACS) containing 25 mM HEPES and 0.85 mg/ml collagenase type Ⅱ (Gibco™, 17101015). After digestion, the liver was dissected and cells were released and filtered through a 70 μM cell strainer and centrifuged at 1,100 g. Isolated primary hepatocytes were resuspended and then plated into 12-well plate coated with rat tail collagen I (Solarbio, C8062) at a density of 2×10^5 per well.

Fibro-adipogenic progenitors (FAPs) were isolated following previously reported protocol with minor adjustments [31]. Briefly, tibialis anterior (TA) was excised from 8-week-old male C57BL/6J mice, transferred into precooled PBS, carefully removed non-muscle tissue, minced with scissors,

https://doi.org/10.1017/anr.2024.26 Published online by Cambridge University Press

and then digested with 1 mg/ml type II collagenase (Gibco™, 17101015) at 37°C for 60 min. Muscle slurries were filtered through a cell strainer (70 μm) to remove large pieces and then centrifuged at 1,100 g for 4 min. After being washed twice with PBS, the cell pellets were incubated with red blood cell lysis buffer (Beyotime Biotechnology, C3702) for 1 min, followed by centrifugation at 1,100 g for 4 min. Isolated FAPs were resuspended and then plated into 10 cm dish. Floating cells were removed 4 h later, and fresh culture medium was added.

2.4. Cell culture and differentiation

Mouse primary hepatocytes were cultured in Williams E media (Procell Life Science&Technology, PM151211) containing 10% fetal bovine serum (FBS, Gibco™, 10099141), 2 mM Glutamine (Procell Life Science&Technology, PB180420), and 1% penicillin-streptomycin (NEST Biotechnology, 211092) in a humidified atmosphere at 37°C with 5% CO_2.

FAPs were cultured in Dulbecco's Modified Eagle Medium/Nutrient Mixture F-12 (DMEM/F12, Gibco™, 11320033) containing 15% FBS (Gibco™, 10099141) and 1% penicillin-streptomycin (Gibco™, 15140122) in a humidified atmosphere at 37°C with 5% CO_2. To induce differentiation, after 2 days post-confluence, differentiation of FAPs were induced using an induction medium containing 1 μM dexamethasone (Sigma-Aldrich, D4902), 500 μM IBMX (Sigma-Aldrich, I5879), 5 μg/ml insulin (Solarbio, I8040), and 0.5 μmol/l rosiglitazone (Sigma-Aldrich, PHR2932) for 3 days, followed by a differentiation medium containing 5 μg/ml insulin. Fresh differentiation medium was replaced every 2 days until cells were ready for harvest, typically around day 8.

2.5. Cell transfection

For knockdown of *Fto*, the small interfering RNA (siRNA) were transfected using Lipofectamine RNAiMAX (Invitrogen, 13778030), according to the manufacturer's instructions. The siRNAs were ordered from GenePharma and the sequences are as follows (5'-3').

Negative control siRNA: UUCUCCGAACGUGUCACGUTT.

Mouse *Fto* siRNA: TTAAGGTCCACTTCATCATCGCAGG.

2.6. Bodipy staining

Cells were washed twice with PBS and stained with 1 μg/ml Bodipy 493/503 (Invitrogen, D3922) at 37°C in the dark for 30 min. Subsequently, cells were washed 3 times with PBS, counterstained with Hoechst 33342 (Yeasen, 40732ES03) at 37°C in the dark for 10 min, and finally washed 3 times with PBS again. A fluorescence microscope was used to observe and photograph in a

https://doi.org/10.1017/anr.2024.26 Published online by Cambridge University Press

darkened microscopy room.

2.7. Quantitative real-time PCR (qPCR)

According to the instructions, RNA from tissues or cells was extracted using FreeZol Reagent (Vazyme, R71102), and then reverse transcribed into complementary DNA (cDNA) by SPARKscript Ⅱ One Step RT-PCR Kit (Shandong Sparkjade Biotechnology Co., Ltd., AG0402). Quantitative real-time PCRs were performed on the ABI Step-One Plus^{TM} Real-Time PCR System (Applied Biosystems) using SYBR Green Fast qPCR Mix (ABclonal, RK21203). Relative mRNA abundance of gene was calculated by the $2^{-\Delta\Delta Ct}$ method, with β-actin used as an internal control.

Table 2 Primer sequences used in this study.

Gene	Forward primer (5'-3')	Reverse primer (3'-5')
p-β-actin	AGTTGAAGGTGGTCTCGTGG	TGCGGGACATCAAGGAGAAG
p-FABP4	GCGACGGTGCCTCTGGTAGT	CGCAAGACGGCGGATTTA
p-CEBPα	GGTGGACAAGAACAGCAACG	AGGCACCGGAATCTCCTAGT
p-PPARγ	TGACCATGGTTGACACCG	AAGCATGAACTCCATAGTGG
p-METTL3	AGTGGCTTTTCATCTTGGCTCTA	AGTGGCTTTTCATCTTGGCTCTA
p-METTL14	GGATGTAGGTTTGGCCGACA	GGGGGTTCCAGAAGAATCACA
p-FTO	ATAGCAGCAGCATGAAGCGA	CAGCTGCCACTGCTGATAGA
p-ALKBH5	CCAGTTCAAGCCTATCCGGG	GCGCATCTAACCTTGTCTTCC
m-β-actin	CTGGACTACCTCCTGTCTGCT	CCCCCAAGGTGAAGGGTAAAC
m-FABP4	GTGTGATGCCTTTGTGGGAAC	CCTGTCGTCTGCGGTGATT
m-CEBPα	GGTTTCGGGTCGCTGGATCTCTAG	ACGGCCTGACTCCCTCATCTTAGAC
m-PPARγ	GACCACTCGCATTCCTT	CCACAGACTCGGCACTC
m-METTL3	AGTGGCTTTTCATCTTGGCTCTA	GCTGTTTCTTATGGGCCTGGA
m-METTL14	CGGCTTTACTCCTCGGTAGC	TCACCCACCCTGAGCAAAAG
m-FTO	GAGCAGCCTACAACGTGACT	GAAGCTGGACTCGTCCTCAC
m-ALKBH5	GCTGTGGTGAGAGAAAGCCT	AGTGGGCAAACACAAGTCCA

2.8. Western blot

Protein in tissues or cells were extracted using the cell total protein extraction kit (Solarbio, BC3710). Quantification was performed using the bicinchoninic acid (BCA) protein concentration assay kit (Solarbio, PC0020). Samples were separated on 10% SDS-PAGE gels and blotted onto PVDF membrane (Millipore, IPVH00010). After blocking with 5% skim milk (Solarbio, D8340) at room temperature for 1 h, the membranes were incubated with rabbit anti-FTO (Proteintech,

https://doi.org/10.1017/anr.2024.26 Published online by Cambridge University Press

27226-1-AP) at 4°C overnight, and subsequently incubated with HRP-conjugated secondary antibodies (Biosharp, BL003A) at room temperature for 1 h. The membranes were visualized with Super ECL Plus (US EVERBRIGHT, S6009L).

2.9. mRNA isolation and m^{6}A dot blot assays

mRNA was purified from total RNA using two rounds of polyA-tail purification with the Dynabeads® mRNA DIRECT™ kit (Thermo Fisher Scientific, 61012) and quantified with a Qubit Fluorometer (Thermo Fisher Scientific, Q33216).

Dot blot procedure was modified according to previously published researches [32,33]. 3 μl samples containing mRNA (600 ng) were denatured by heating at 65°C for 5 min to disrupt secondary structures, spotted on Amersham Hybond-N+ membrane (GE Healthcare, RPN203B), and then UV crosslinked (twice, 1200 J/cm^2). After blocking with 5% skim milk (Solarbio, D8340) at room temperature for 1 h, the membrane was incubated with anti-m^{6}A antibodies (Huabio, HA721152) at 4°C overnight, and subsequently incubated with HRP-conjugated secondary antibodies (Biosharp, BL003A) at room temperature for 1 h. The membranes were visualized with Super ECL Plus (US EVERBRIGHT, S6009L). After exposure, the membrane was stained with 0.02% methylene blue dissolved in 0.3 M sodium acetate (Sigma-Aldrich, M9140) to verify the mRNA were loaded equally.

2.10. Total triglyceride (TG) detection

The TG levels of mouse TA samples were measured by using commercial kit (Nanjing Jiancheng, A110-1-1) according to the manufacture's protocol.

2.11. Flow cytometry

Cells were harvested and washed with PBS, fixed in 70% cold ethanol, and stored at -20°C overnight (at least 18 h). Fixed cells were washed twice and incubated with 0.5 ml FxCycle™PI/RNase Solution. After incubation, cells were subjected to flow cytometer (Becton Dickinson). Data of cell cycle distribution were analyzed by ModFit LT 5.0 Software [34].

2.12. Statistical analysis

Significance between groups was analyzed using unpaired Student's t-test or one-way ANOVA after testing for homogeneity of variances with Levene's test using GraphPad Prism 8. All data were presented as the mean ± standard deviation (SD) and $P < 0.05$ was considered statistically significant.

https://doi.org/10.1017/anr.2024.26 Published online by Cambridge University Press

3. Results

3.1. Betaine promotes intramuscular fat deposition *in vivo*

To assess the role of betaine on intramuscular fat (IMF) deposition *in vivo*, Duroc × Landrace × Yorkshire (DLY) crossbred finishing pigs were randomly assigned to two groups and fed either a basal diet (CTL) or a basal diet supplemented with 2500 mg/kg betaine (BET) for a duration of 40 days (Fig. 1A). Remarkably, the inclusion of betaine in diet dramatically elevated the IMF content in the *longissimus dorsi* muscle (Fig. 1D), despite comparable average daily weight gain (Fig. 1B) and carcass weight (Fig. 1C). To further determine the promoting effect of betaine on IMF deposition, male C57BL/6J mice were subjected to a normal chow diet (NCD) or a NCD plus 2% betaine (water supplementation, Bet) (Fig. 1E). As anticipated, dietary betaine treatment didn't result in any notable impact on body weight (Fig. 1F-H) or daily average food consumption (Fig. 1I) of mice. However, it markedly increased IMF accumulation in the tibialis anterior muscle of mice, as indicated by Bodipy staining (Fig. 1J). Consistently, the TG content (Fig. 1K), as well as the gene expression of lipid metabolism master regulators including fatty acid binding protein 4 (FABP4), CCAAT enhancer-binding protein alpha (CEBPα), and peroxisome proliferator activated receptor gamma (PPARγ) (Fig. 1L), were significantly upregulated owing to betaine intervention. All these findings demonstrate that betaine can lead to higher IMF deposition without exacerbating body weight *in vivo*.

3.2. Betaine facilitates IMF formation after being metabolized through the liver

Subsequently, porcine intramuscular adipocytes (PIMF) and mouse fibro/adipogenic progenitors (FAPs) were extracted as cellular models for further study *in vitro*. Nevertheless, it was noteworthy that intervening directly with betaine revealed no discernible impact on the polyester differentiation of PIMF (Fig. 2A) or FAPs (Fig. 2C). The mRNA expression levels of key adipogenic genes also cannot be significantly altered in such situation (Fig. 2B, D). As extensive research established, the liver is a major location for betaine metabolism, and the metabolic activation within the liver plays a vital role in enabling betaine carry out its physiological functions effectively [35]. In light of this, we treated FAPs with cultural supernatants of betaine-treated hepatocytes (Fig. 2E) and surprisingly observed enhanced the differentiation of polyester into intramuscular adipocytes (Fig. 2F), along with increased mRNA expression levels of *Fabp4*,

https://doi.org/10.1017/anr.2024.26 Published online by Cambridge University Press

Cebpα, and *Pparγ* (Fig. 2G). Taken together, betaine does not directly facilitate IMF deposition, instead, its influence is manifested post-metabolism in liver. Further in-depth analysis is needed to understand how betaine promotes IMF deposition via liver metabolism.

3.3. Betaine stimulates the production of NADPH in the liver, thereby elevating IMF content

To investigate the alterations in hepatic metabolism following betaine administration, we analyzed the effects of betaine on liver transcriptome of wild-type mice, utilizing previously documented RNA sequencing (RNA-seq) data [36]. A total of 1730 genes exhibited significant changes due to betaine supplementation: 923 genes were distinctly upregulated, while 807 genes were notably downregulated in betaine-treated mice compared with the control group (Fig. 3A). GO annotation classification analysis of upregulated genes clearly indicated a notable enrichment in pathways associated with nicotinamide adenine dinucleotide phosphate (NADPH) production (Fig. 3B). And it's noteworthy that betaine could obviously increase the NADPH content in cultural supernatants of hepatocytes (Fig. 3C). According to this discovery, we postulated that betaine may enhance the production of NADPH in liver, subsequently leading to an increase in IMF accumulation. To explore this possibility, we detected NADPH content and found that betaine treatment obviously elevated the levels of NADPH in liver, serum, and skeletal muscle of both porcine (Fig. 3D, E) and murine subjects (Fig. 3F, G). What's more, the differentiation of polyester into intramuscular adipocytes was enhanced in a dose-dependent manner with the exogenous addition of varying concentrations of NADPH (0, 300, 600 μM) to PIMF (Fig. 3H) or FAPs (Fig. 3J). The mRNA expression levels of critical adipocyte differentiation markers corroborated this finding (Fig. 3I, K). In summary, the data presented suggest that betaine promotes the formation of IMF by stimulating the production of NADPH.

3.4. NADPH promotes the cloning and proliferation process of intramuscular adipocytes

Elucidating the potential mechanisms through which NADPH enhances IMF content is the next question we attempted to decipher. In this regard, according to available RNA-seq data, 1702 genes showed differential expression in FAPs induced by adipogenesis compared with the control group (Fig. 4A). Through Reactome analysis (Fig. 4B), KEGG analysis (Fig. 4C), and GO annotation classification analysis (Fig. 4D), we noted that upregulated genes were dramatically enriched in mitotic clonal expansion (MCE)-related processes, such as DNA replication and cell cycle. MCE serves as a critical prerequisite for the differentiation of 3T3-L1 preadipocytes into

https://doi.org/10.1017/anr.2024.26 Published online by Cambridge University Press

mature adipocytes, marking it as the most significant event in the early stages of the program [37,38]. Whether NADPH modulates IMF deposition through regulating the MCE process? We then analyzed the cell cycle distribution of control and betaine-treated PIMF (Fig. 4E, F) or FAPs (Fig. 4G, H) via flow cytometry to substantiate this hypothesis. The results revealed that NADPH could effectively decrease the relative proportion of cells in G0-G1 phase, suggesting that betaine-induced NADPH facilitates the cloning and proliferation process of intramuscular adipocytes to further enhance IMF deposition. Whereas, so far, our understanding of the precise mechanisms underlying the promotion of NADPH on the cell cycle process is largely unknown.

3.5. Betaine and NADPH reduce m^{6}A modification via accelerating FTO expression

N^6-methyladenosine (m^{6}A) represents the most widespread and abundant mRNA modification in eukaryotic organisms. It serves as a key regulatory pathway for various biological events, encompassing cell differentiation and metabolic reprogramming [39]. What's more, our previous work, along with that of others, has provided insight into the crucial role of m^{6}A modification in the processes of adipogenesis in liver and inguinal white adipose tissue (iWAT) [33,38,40,41]. These pieces of evidence collectively prompted us to hypothesize whether the promoter function of betaine-induced NADPH on the cell cycle process in intramuscular adipocytes may be linked to m^{6}A methylation as well. To determine this possibility, total m^{6}A-modified mRNA levels were detected using m^{6}A dot blot. Attractively, betaine intervention resulted in a dramatical reduction of overall m^{6}A levels in skeletal muscle, irrespective of whether the subjects were pigs (Fig. 5A) or mice (Fig. 5B). Coinciding with our *in vivo* data, m^{6}A levels were also lower in PIMF (Fig. 5C) or FAPs (Fig. 5D) following NADPH treatment compared with the control. Owing to the abundance of m^{6}A on mRNA being determined by the dynamic interplay between demethylases (erasers, FTO and ALKBH5) and methyltransferases (writers, METTL3 and METTL14) enzyme families, we subsequently examined and identified FTO as the key m^{6}A regulator contributes to the mitigated m^{6}A levels (Fig. 5E-H). Intervening directly with betaine didn't cause any significant alteration on overall m^{6}A levels of PIMF (Fig. 5I, K) or FAPs (Fig. 5J, L). To sum up, betaine and NADPH can downregulate FTO-mediated m^{6}A methylation *in vivo* and *in vitro*.

3.6. FTO is essential for NADPH-promoted MCE process and further IMF deposition

So, whether the decreased m^{6}A modification was a contributing factor that further affects the MCE process and ultimately the IMF content? To explore this, we then conducted loss-of-function

https://doi.org/10.1017/anr.2024.26 Published online by Cambridge University Press

studies by perturbing FTO to assess the mediator of m^6A modification. Quantitative PCR and Western blot analyses demonstrated that silencing of FTO markedly attenuated the elevated mRNA and protein abundance of FTO in NADPH-treated PIMF (Fig. 6A, B) or FAPs (Fig. 6D, E). Consistently, exogenous addition of NADPH had no significant impact on cellular m^6A levels with the depletion of FTO (Fig. 6C, F). Regarding the final IMF deposition, it was discovered that interfering with FTO expression effectively impede the role of NADPH in promoting adipogenic differentiation of intramuscular adipocytes (Fig. 6G, I) and significantly reduced the mRNA expression of adipocyte differentiation markers FABP4, C/EBPα, and PPARγ (Fig. 6H, J). Additionally, the NADPH-facilitated cell cycle process of PIMF (Fig. 6K, L) and FAPs (Fig. 6M, N) were also inhibited in the absence of FTO. These observations collectively substantiate that FTO acts as a vital mediator in NADPH-promoted MCE process and subsequent IMF accumulation within intramuscular adipocytes.

4. Discussion

Appropriate deposition of IMF is the most vital factor determining pork quality in livestock production and also holds critical medical implications for human health. Betaine, one of non-essential amino acids, has demonstrated considerable potential as a nutritional strategy for regulating intramuscular adipogenesis, although its exact efficacy and underlying mechanisms still remain subjects of ongoing debate and investigation. Here in this study, we clarify the promoting effect of betaine on IMF deposition and further delineate a novel NADPH-m^6A-MCE axis that enhances the adipogenic differentiation of intramuscular adipocytes.

Early in 2002, Lawrence et al. reported that feeding diets with 1.25 g/kg supplemental betaine had no statistically significant effect on IMF content in finishing swine [42]. Whereas, different from this notion, Albuquerque et al. discovered that long-term 1g/kg betaine intervention can selectively promote muscle lipogenesis while not affecting other physical and chemical characteristics in pigs [43]. Our prior research published in 2018 also indicated that 10mM betaine markedly facilitates cellular lipid accumulation in C2C12 (C2 mouse myoblast cell line) through inhibition of ERK1/2 signaling on the late adipogenic stage [15]. To thoroughly and comprehensively examine this controversial issue, we undertook new experimental investigations based on porcine, murine, and cellular models, which confirmed the promoting effect of betaine on intramuscular adipogenesis.

https://doi.org/10.1017/anr.2024.26 Published online by Cambridge University Press

However, our available findings are not yet able to sufficiently elucidate the discrepancies among existing studies. Differences in experimental models and designs, such as variations in treatment dosage or duration, may serve as potential explanations.

Another important finding of our work, to the best of our knowledge, is the first demonstration showing that betaine cannot directly modulate IMF deposition but rather does so in a liver-dependent manner. Liver is a major site for betaine metabolism, bridging the dynamic cross-talk between betaine and peripheral target tissues. Here we innovatively found that intervening with culture supernatants derived from betaine-treated hepatocytes, rather than the direct use of betaine, results in higher cellular IMF content through regulating pathways associated with NADPH production. How betaine elevates NADPH levels is the upstream regulatory mechanisms that is not addressed in this study but merits further in-depth investigation. As for this matter, it is noteworthy that betaine has been recognized as a participant in one-carbon metabolism [22]. The folate cycle, which is part of one-carbon metabolism, is an important source of NADPH in mammals, accounting for 40% to its overall production [44]. Exploring from this perspective perhaps provide insights into the fundamental mechanisms involved.

Previous publications, including our own, have established that MCE functions as an essential prerequisite for 3T3-L1 preadipocytes to differentiate into mature adipocytes [33,34,37,45]. Considering this, we direct our attention to the cell cycle and present compelling evidence indicating that NADPH can significantly promote the cloning and proliferation process in intramuscular adipocytes to facilitate IMF formation. What's more, our results substantiate the important function of FTO-mediated m^6A modification in this process. CCNA2 and CDK2 are key regulators of early mitotic events and play vital roles in cell cycle regulation and the G1/S phase transition [46]. Therefore, subsequent studies also should be conducted to screen out which gene(s) involved in NADPH-altered MCE process.

5. Conclusion

In summary, we show that betaine enhances intramuscular adipogenesis by promoting MCE process in an NADPH-FTO-m^6A coordinated manner. Betaine supplementation elevates NADPH levels in liver, circulation, and skeletal muscle, which subsequently diminishes FTO-mediated m^6A modification in intramuscular adipoctyes, thereby facilitating the cloning and proliferation of

https://doi.org/10.1017/anr.2024.26 Published online by Cambridge University Press

intramuscular adipocytes and the differentiation of polyester in intramuscular adipocytes. Our work expands our understanding of the regulatory function of betaine in IMF deposition and sheds light on the molecular mechanisms underlying its modulation.

Acknowledgements

This work was supported by the National Key R&D Program of China (2023YFD1301303), the National Natural Science Foundation of China (32330098), and the Science and technology innovation leading talent project of Zhejiang Province (2022R52023).

Authors' contributions

Jiaqi Liu, Tongyudan Yang, Yuxi Liu, Youhua Liu, and Chaoqun Huang performed experimental work under the supervision of Xinxia Wang. Jiaqi Liu, Tongyudan Yang, and Yuxi Liu were the main contributors in the conduct of study, data collection and analysis, data interpretation. Jiaqi Liu and Tongyudan Yang wrote and revised the manuscript. Jiaqi Liu and Tongyudan Yang contributed equally to this work. All the authors have read and approved the published version of the manuscript.

Declaration of Competing interests

The authors declare that they have no competing interests.

Data availability

All public RNA profile data analyzed during the study could acquire from the Gene Expression Omnibus (GEO, http://www.ncbi.nlm.nih.gov/geo/). The datasets used and/or analysed during the current study are available from the corresponding author on reasonable request.

References

1. Liu, K. et al. Melatonin reduces intramuscular fat deposition by promoting lipolysis and increasing mitochondrial function. *Journal of Lipid Research* **60**, 767-782 (2019).
2. Lee, E.C. et al. Ergogenic effects of betaine supplementation on strength and power performance. *J Int Soc Sports Nutr* **7**, 27 (2010).
3. Yu, X. et al. Neonatal vitamin A administration increases intramuscular fat by promoting angiogenesis and preadipocyte formation. *Meat Science* **191**, 108847 (2022).
4. Font-i-Furnols, M., Tous, N., Esteve-Garcia, E. & Gispert, M. Do all the consumers accept marbling in the same way? The relationship between eating and visual acceptability of pork with different intramuscular fat content. *Meat Science* **91**, 448-453 (2012).
5. Goodpaster, B.H., Theriault, R., Watkins, S.C. & Kelley, D.E. Intramuscular lipid content is

increased in obesity and decreased by weight loss. *Metabolism, clinical and experimental* **49**, 467-472 (2000).

6. Prior, S.J. et al. Reduction in midthigh low-density muscle with aerobic exercise training and weight loss impacts glucose tolerance in older men. *J Clin Endocrinol Metab* **92**, 880-6 (2007).

7. Gao, S. et al. ZAG alleviates HFD-induced insulin resistance accompanied with decreased lipid depot in skeletal muscle in mice. *Journal of Lipid Research* **59**, 2277-2286 (2018).

8. Zhao, G. et al. Betaine in Inflammation: Mechanistic Aspects and Applications. *Front Immunol* **9**, 1070 (2018).

9. Dobrijević, D. et al. Betaine as a Functional Ingredient: Metabolism, Health-Promoting Attributes, Food Sources, Applications and Analysis Methods. *Molecules* **28**, 4824 (2023).

10. Veskovic, M. et al. Betaine modulates oxidative stress, inflammation, apoptosis, autophagy, and Akt/mTOR signaling in methionine-choline deficiency-induced fatty liver disease. *European Journal of Pharmacology* **848**, 39-48 (2019).

11. Abd El-Ghany, W.A. & Babazadeh, D. Betaine: A Potential Nutritional Metabolite in the Poultry Industry. *Animals* **12**, 2624 (2022).

12. Idriss, A.A. et al. Prenatal betaine exposure modulates hypothalamic expression of cholesterol metabolic genes in cockerels through modifications of DNA methylation. *Poultry science* **96**, 1715-1724 (2017).

13. Kathirvel, E. et al. Betaine improves nonalcoholic fatty liver and associated hepatic insulin resistance: a potential mechanism for hepatoprotection by betaine. *Am J Physiol Gastrointest Liver Physiol* **299**, G1068-77 (2010).

14. Li, J.M. et al. Betaine recovers hypothalamic neural injury by inhibiting astrogliosis and inflammation in fructose-fed rats. *Molecular Nutrition & Food Research* **59**, 189-202 (2015).

15. Wu, W. et al. Betaine promotes lipid accumulation in adipogenic-differentiated skeletal muscle cells through ERK/PPARγ signalling pathway. *Molecular and Cellular Biochemistry* **447**, 137-149 (2018).

16. Madeira, M.S. et al. The combination of arginine and leucine supplementation of reduced crude protein diets for boars increases eating quality of pork1. *Journal of animal science* **92**, 2030-2040 (2014).

17. Ma, X. et al. Effect of amino acids and their derivatives on meat quality of finishing pigs. *Journal of Food Science and Technology* **57**, 404-412 (2020).

18. Madeira, M.S. et al. Effect of betaine and arginine in lysine-deficient diets on growth, carcass traits, and pork quality1. *Journal of animal science* **93**, 4721-4733 (2015).

19. Wu, R. & Wang, X. Epigenetic regulation of adipose tissue expansion and adipogenesis by N^6-methyladenosine. *Obesity Reviews* **22**(2021).

20. Chen, M. & Wong, C. The emerging roles of N^6-methyladenosine (m^6A) deregulation in liver carcinogenesis. *Molecular Cancer* **19**(2020).

21. Gong, H., Gong, T., Liu, Y., Wang, Y. & Wang, X. Profiling of N6-methyladenosine methylation in porcine longissimus dorsi muscle and unravelling the hub gene ADIPOQ promotes adipogenesis in an m6A-YTHDF1–dependent manner. *Journal of Animal Science and Biotechnology* **14**(2023).

22. Wang, C., Ma, C., Gong, L., Dai, S. & Li, Y. Preventive and therapeutic role of betaine in liver disease: A review on molecular mechanisms. *Eur J Pharmacol* **912**, 174604 (2021).

23. Fu, R. et al. Long-Term Dietary Supplementation with Betaine Improves Growth

https://doi.org/10.1017/anr.2024.26 Published online by Cambridge University Press

Performance, Meat Quality and Intramuscular Fat Deposition in Growing-Finishing Pigs. *Foods* **12**, 494 (2023).
24. Turck, D. et al. Safety of betaine as a novel food pursuant to Regulation (EU) 2015/2283. *EFSA Journal* **17**(2019).
25. Liu, J. et al. Betaine alleviates nonalcoholic fatty liver disease (NAFLD) via a manner involving BHMT/FTO/m6A/ PGC1α signaling. *The Journal of Nutritional Biochemistry* **134**, 109738 (2024).
26. Chen, W. et al. Betaine prevented high-fat diet-induced NAFLD by regulating the FGF10/AMPK signaling pathway in ApoE−/− mice. *European Journal of Nutrition* **60**, 1655-1668 (2021).
27. Lv, S. et al. Betaine supplementation attenuates atherosclerotic lesion in apolipoprotein E-deficient mice. *European Journal of Nutrition* **48**, 205-212 (2009).
28. Xu, Z. et al. Single-cell RNA sequencing and lipidomics reveal cell and lipid dynamics of fat infiltration in skeletal muscle. *Journal of Cachexia, Sarcopenia and Muscle* **12**, 109-129 (2021).
29. Mahdy, M.A.A. Glycerol-induced injury as a new model of muscle regeneration. *Cell and Tissue Research* **374**, 233-241 (2018).
30. Charni-Natan, M. & Goldstein, I. Protocol for Primary Mouse Hepatocyte Isolation. *STAR protocols* **1**, 100086-100086 (2020).
31. Kang, X. et al. Exercise-induced Musclin determines the fate of fibro-adipogenic progenitors to control muscle homeostasis. *Cell Stem Cell* **31**, 212-226.e7 (2024).
32. Shen, L., Liang, Z. & Yu, H. Dot Blot Analysis of N6-methyladenosine RNA Modification Levels. *BIO-PROTOCOL* **7**(2017).
33. Huang, C. et al. Branched-chain amino acids prevent obesity by inhibiting the cell cycle in an NADPH-FTO-m^{6}A coordinated manner. *The Journal of Nutritional Biochemistry* (2023).
34. Liao, X. et al. Metformin combats obesity by targeting FTO in an m^{6}A-YTHDF2-dependent manner. *Journal of drug targeting* **30**, 983-991 (2022).
35. Ejaz, A. et al. Dietary betaine supplementation increases Fgf21 levels to improve glucose homeostasis and reduce hepatic lipid accumulation in mice. *Diabetes (New York, N.Y.)* (2016).
36. Huang, T. et al. Integrated Transcriptomic and Translatomic Inquiry of the Role of Betaine on Lipid Metabolic Dysregulation Induced by a High-Fat Diet. *Frontiers in Nutrition* **8**(2021).
37. Chang, E. & Kim, C.Y. Natural Products and Obesity: A Focus on the Regulation of Mitotic Clonal Expansion during Adipogenesis. *Molecules (Basel, Switzerland)* **24**, 1157 (2019).
38. Wu, R. et al. Epigallocatechin gallate targets FTO and inhibits adipogenesis in an mRNA m6A-YTHDF2-dependent manner. *International Journal of Obesity* **42**, 1378-1388 (2018).
39. Li, Y. et al. RNA *N*^{6}-methyladenosine: a promising molecular target in metabolic diseases. *Cell & Bioscience* **10**(2020).
40. Chen, Y. et al. Curcumin prevents obesity by targeting TRAF4-induced ubiquitylation in m^{6}A-dependent manner. *EMBO Reports* (2021).
41. Wang, X. et al. m6A mRNA methylation controls autophagy and adipogenesis by targeting Atg5 and Atg7. *Autophagy* **16**, 1221-1235 (2020).
42. Lawrence, B.V., Schinckel, A.P., Adeola, O. & Cera, K. Impact of betaine on pig finishing performance and carcass composition1. *Journal of Animal Science* **80**, 475–482 (2002).
43. Albuquerque, A. et al. Long-term betaine supplementation regulates genes involved in lipid and cholesterol metabolism of two muscles from an obese pig breed. *Meat Science* **124**, 25-33

https://doi.org/10.1017/anr.2024.26 Published online by Cambridge University Press

(2017).
44. Fan, J. et al. Quantitative flux analysis reveals folate-dependent NADPH production. *Nature* **510**, 298-302 (2014).
45. Kim, M. et al. Apigenin isolated from Daphne genkwa Siebold et Zucc. inhibits 3T3-L1 preadipocyte differentiation through a modulation of mitotic clonal expansion. *Life Sciences* **101**, 64-72 (2014).
46. Tang, Q., Otto, T.C. & Lane, M.D. Mitotic Clonal Expansion: A Synchronous Process Required for Adipogenesis. *Proceedings of the National Academy of Sciences - PNAS* **100**, 44-49 (2003).

https://doi.org/10.1017/anr.2024.26 Published online by Cambridge University Press

Figure legends

Figure 1. Betaine promotes intramuscular fat deposition *in vivo*.

(A) Schematic illustration of the experimental design for administering betaine to DLY pigs.

(B) Average daily weight gain of pigs.

(C) Carcass weight of pigs.

(D) IMF content of *longissimus dorsi* muscle from pigs.

(E) Schematic illustration of the experimental design for administering betaine to C57BL/6J mice.

(F) Representative photographs of mice.

(G) Dynamic changes in body weight of mice.

(H) Relative body weight gain of mice at termination of study.

(I) Food intake of mice.

(J) Representative Bodipy staining of TA from mice (scale bar =500 μm).

(K) TG content of TA from mice.

(L) mRNA expression levels of *Fabp4*, *Cebpα*, and *Pparγ* in TA of mice.

$*P < 0.05$, $**P < 0.01$, and $***P < 0.001$.

Figure 2. Betaine facilitates IMF formation after being metabolized through the liver.

(A) Representative Bodipy staining of porcine intramuscular adipocytes (PIMF) treated with betaine or without (scale bar =100 μm).

(B) mRNA expression levels of *FABP4*, *CEBPα*, and *PPARγ* in PIMF treated with betaine or without.

(C) Representative Bodipy staining of fibro-adipogenic progenitors (FAPs) treated with betaine or without (scale bar =100 μm).

(D) mRNA expression levels of *Fabp4*, *Cebpα*, and *Pparγ* in FAPs treated with betaine or without.

(E) Experimental schematic for collecting cultural supernatants of betaine-treated hepatocytes (Bet-Sup) to treat FAPs, with cultural supernatants of betaine-untreated hepatocytes (CTL-Sup) as control.

Schematic illustration of the experimental design for administering betaine to C57BL/6J mice.

(F) Representative Bodipy staining of FAPs treated with CTL-Sup or Bet-Sup (scale bar =100 μm).

https://doi.org/10.1017/anr.2024.26 Published online by Cambridge University Press

(G) Relative mRNA expression levels of *Fabp4*, *Cebpα*, and *Pparγ* in FAPs treated with CTL-Sup or Bet-Sup.

*$P < 0.05$, **$P < 0.01$, and ***$P < 0.001$.

Figure 3. Betaine stimulates the production of NADPH in the liver, thereby elevating IMF content.

(A) Volcano plot displaying differentially expressed genes in the liver transcriptome between control and betaine-treated mice.

(B) GO annotation classification analysis of upregulated genes in the liver transcriptome.

(C) NADPH content in cultural supernatants of hepatocytes treated with betaine or without.

(D) NADPH content in livers and *longissimus dorsi* muscle of pigs.

(E) Serum levels of NADPH in pigs.

(F) NADPH content in livers and TA of mice.

(G) Serum levels of NADPH in mice.

(H) Representative Bodipy staining of PIMF treated with various concentrations of NADPH (scale bar =100 μm).

(I) mRNA expression levels of *FABP4*, *CEBPα*, and *PPARγ* in PIMF treated with NADPH or without.

(J) Representative Bodipy staining of FAPs treated with various concentrations of NADPH (scale bar =100 μm).

(K) Relative mRNA expression levels of *Fabp4*, *Cebpα*, and *Pparγ* in FAPs treated with NADPH or without.

*$P < 0.05$, **$P < 0.01$, and ***$P < 0.001$.

Figure 4. NADPH promotes the cloning and proliferation process of intramuscular adipocytes.

(A) Volcano plot displaying differentially expressed genes in the transcriptome of mouse intramuscular adipocytes induced by adipogenesis.

(B-D) Reactome analysis **(B)**, KEGG analysis **(C)**, and GO annotation classification analysis **(D)** of differentially expressed genes.

(E-F) Flow cytometry analysis of cell cycle progression in PIMF treated with NADPH or without.

(G-H) Flow cytometry analysis of cell cycle progression in FAPs treated with NADPH or without.

https://doi.org/10.1017/anr.2024.26 Published online by Cambridge University Press

Figure 5. Betaine and NADPH reduce m^{6}A modification via accelerating FTO expression.

(A) mRNA m^{6}A modification levels in *longissimus dorsi* muscle of pigs. Methylene blue staining was used as a loading control.

(B) mRNA m^{6}A modification levels in TA of mice. Methylene blue staining was used as a loading control.

(C-D) mRNA m^{6}A modification levels in PIMF **(C)** and FAPs **(D)** treated with NADPH or without. Methylene blue staining was used as a loading control.

(E-F) mRNA expression levels of METTL3, METTL14, FTO, and ALKBH5 in PIMF **(E)** and FAPs **(F)** treated with NADPH or without.

(G-H) Protein expression levels of FTO in PIMF **(G)** and FAPs **(H)** treated with NADPH or without.

(I-J) mRNA m^{6}A modification levels in PIMF **(I)** and FAPs **(J)** treated with betaine or without.

(K-L) mRNA expression levels of METTL3, METTL14, FTO, and ALKBH5 in PIMF **(K)** and FAPs **(L)** treated with betaine or without.

$^*P < 0.05$, $^{**}P < 0.01$, and $^{***}P < 0.001$.

Figure 6. FTO is essential for NADPH-promoted MCE process and further IMF deposition.

(A) mRNA expression levels of *Fto* in *Fto*-silenced or NADPH-treated PIMF.

(B) Protein expression levels of FTO in *Fto*-silenced or NADPH-treated PIMF.

(C) mRNA m^{6}A modification levels in *Fto*-silenced or NADPH-treated PIMF. Methylene blue staining was used as a loading control.

(D) mRNA expression levels of *Fto* in *Fto*-silenced or NADPH-treated FAPs.

(E) Protein expression levels of FTO in *Fto*-silenced or NADPH-treated FAPs.

(F) mRNA m^{6}A modification levels in *Fto*-silenced or NADPH-treated FAPs. Methylene blue staining was used as a loading control.

(G) Representative Bodipy staining of *Fto*-silenced or NADPH-treated PIMF (scale bar =100 μm).

(H) mRNA expression levels of *FABP4*, *CEBPα*, and *PPARγ* in *Fto*-silenced or NADPH-treated PIMF.

(I) Representative Bodipy staining of *Fto*-silenced or NADPH-treated FAPs (scale bar =100 μm).

(J) mRNA expression levels of *FABP4*, *CEBPα*, and *PPARγ* in *Fto*-silenced or NADPH-treated

https://doi.org/10.1017/anr.2024.26 Published online by Cambridge University Press

FAPs.

(K-L) Flow cytometry analysis of cell cycle progression in *Fto*-silenced or NADPH-treated PIMF.

(M-N) Flow cytometry analysis of cell cycle progression in *Fto*-silenced or NADPH-treated FAPs.

*$P < 0.05$, **$P < 0.01$, and ***$P < 0.001$.

Supplementary Information. Relative fluorescence intensity of Bodipy staining

https://doi.org/10.1017/anr.2024.26 Published online by Cambridge University Press

Figure 1

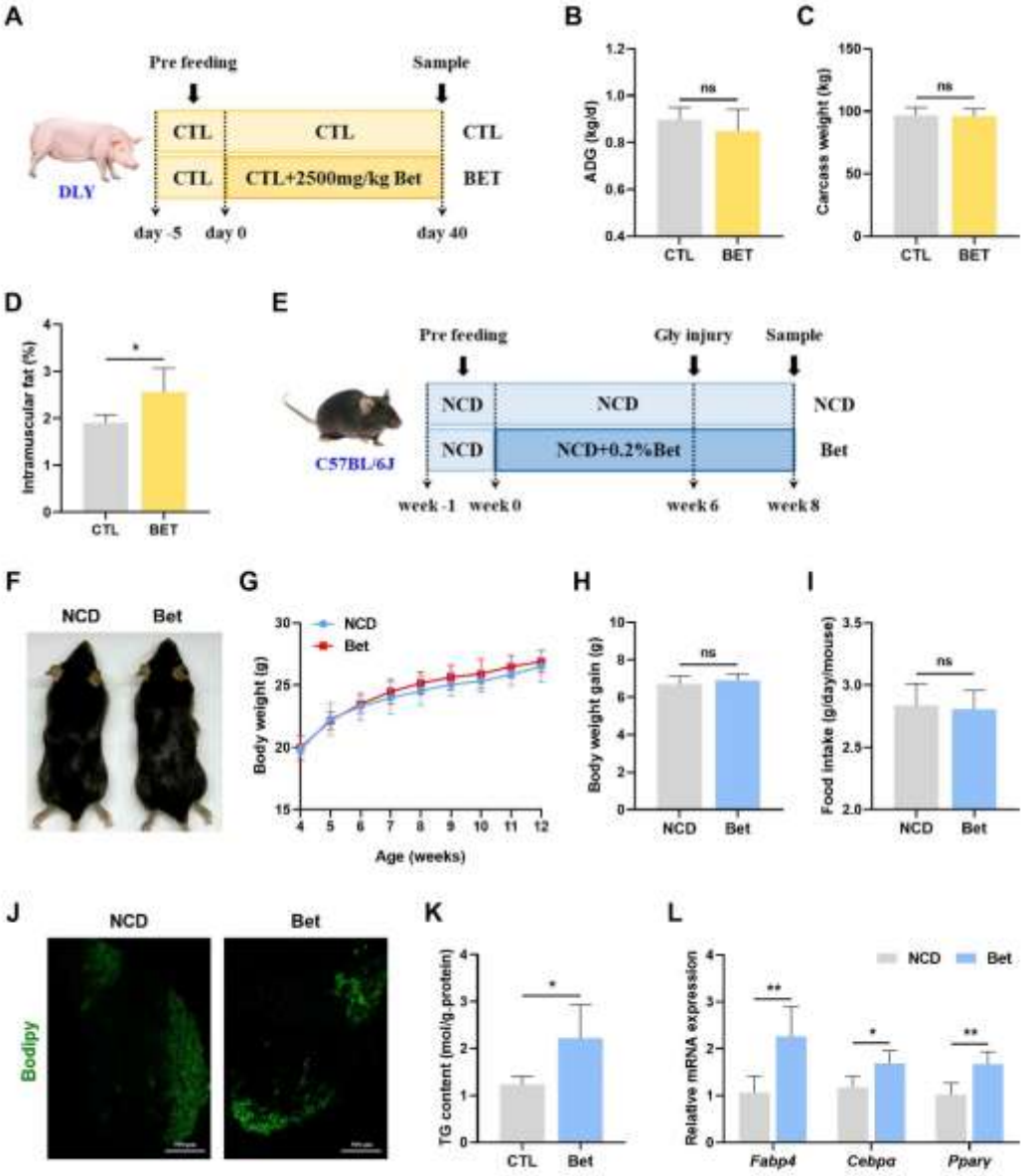

https://doi.org/10.1017/anr.2024.26 Published online by Cambridge University Press

Figure 2

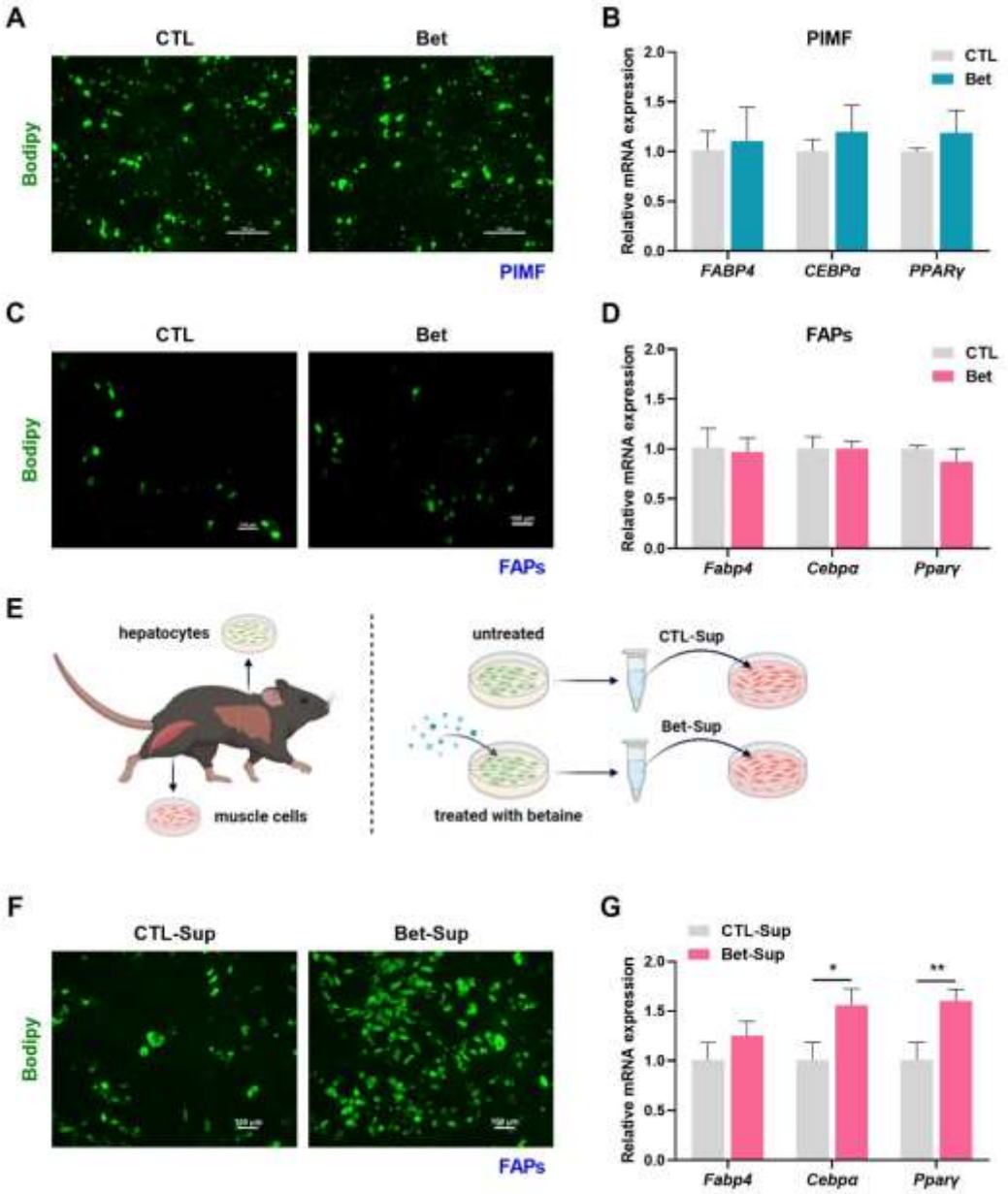

https://doi.org/10.1017/anr.2024.26 Published online by Cambridge University Press

Figure 3

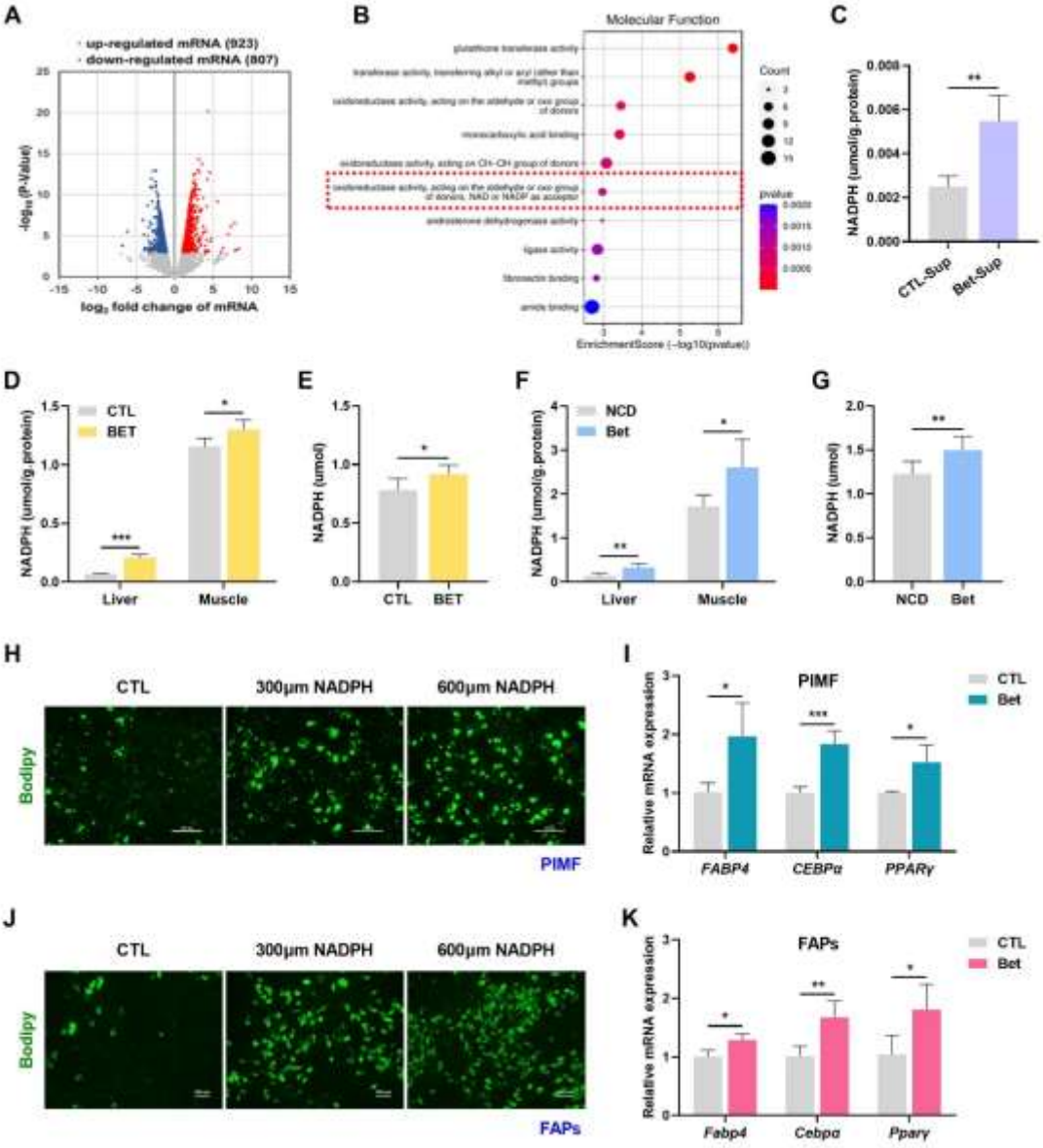

https://doi.org/10.1017/anr.2024.26 Published online by Cambridge University Press

Figure 4

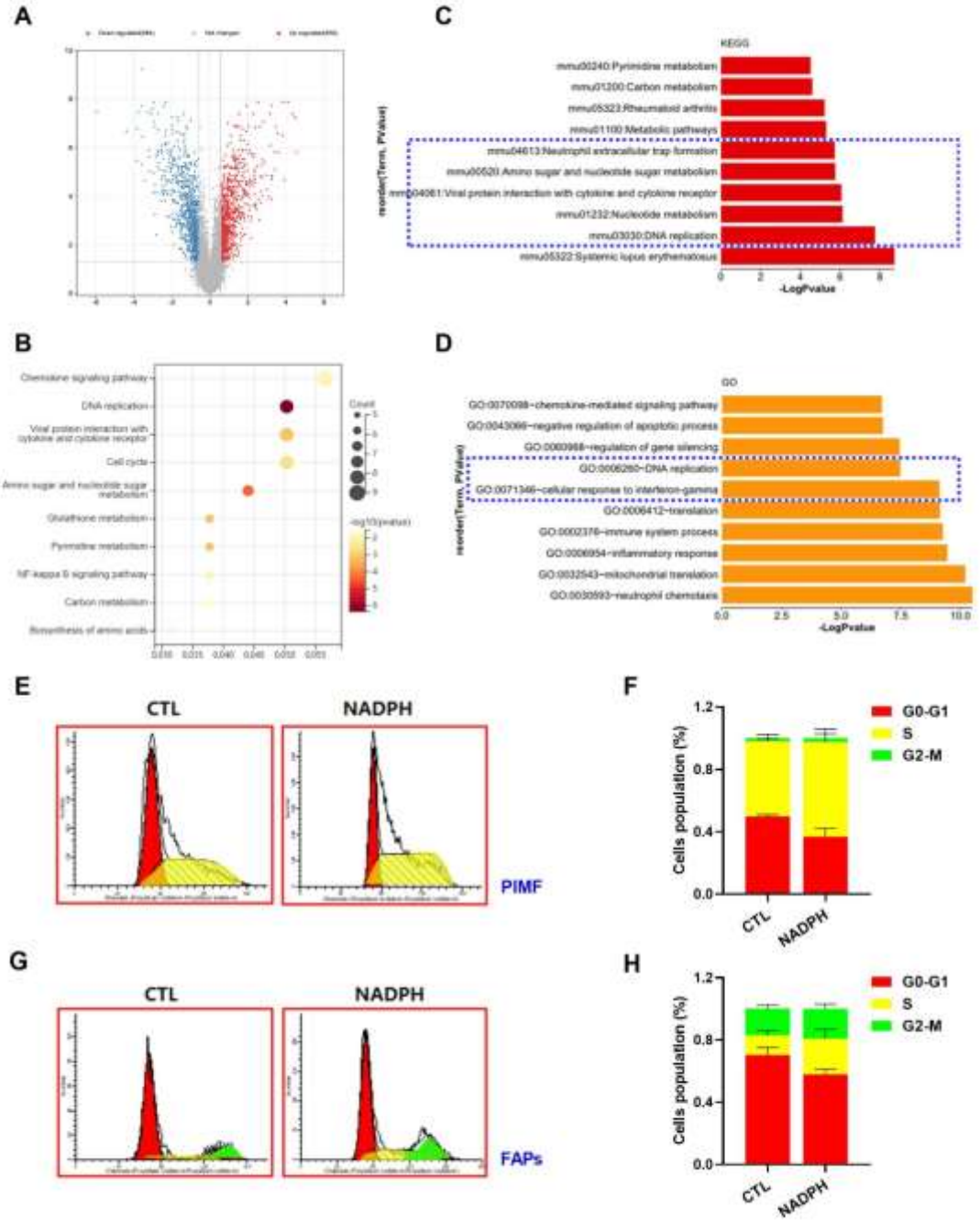

https://doi.org/10.1017/anr.2024.26 Published online by Cambridge University Press

Figure 5

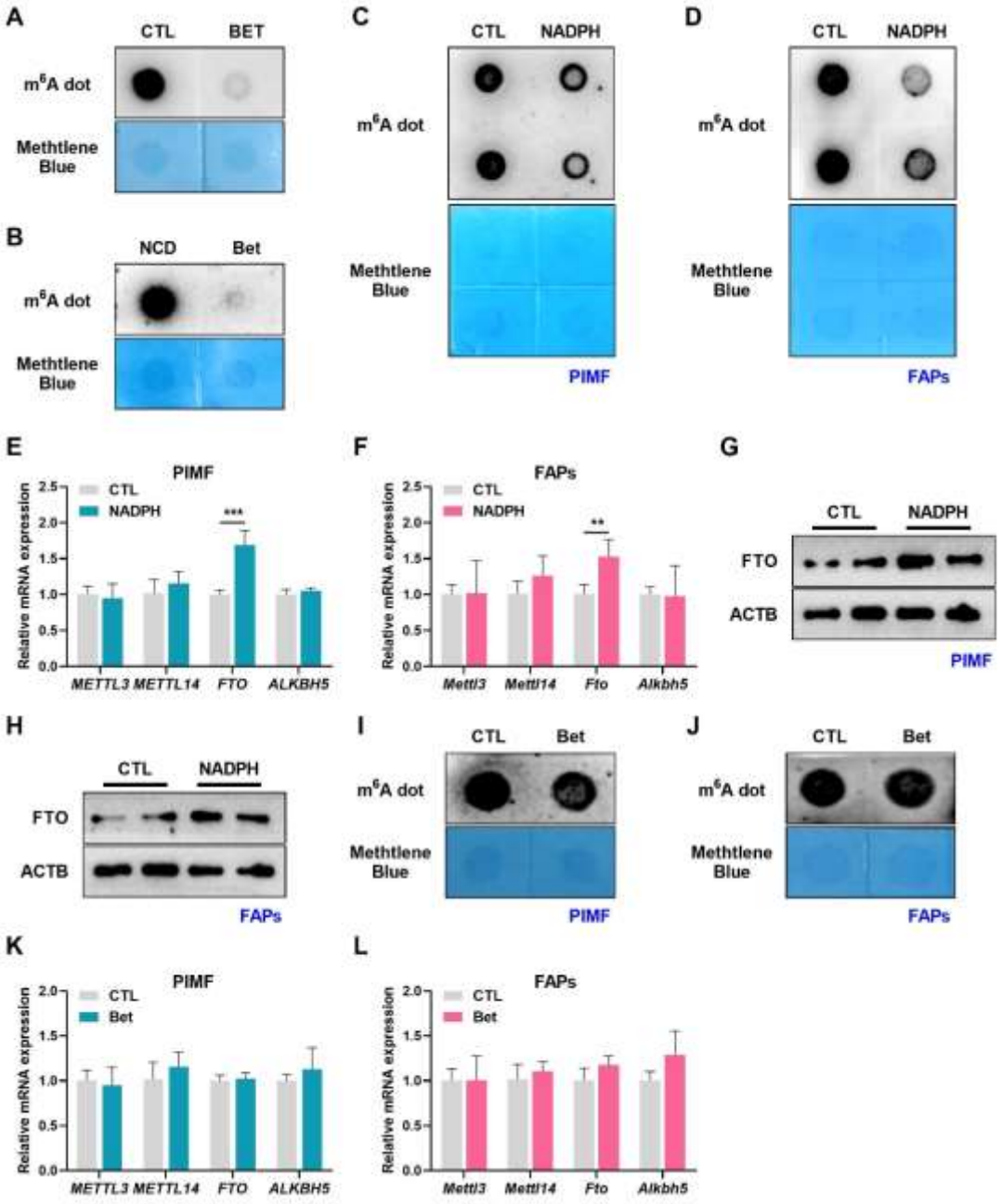

https://doi.org/10.1017/anr.2024.26 Published online by Cambridge University Press

Figure 6

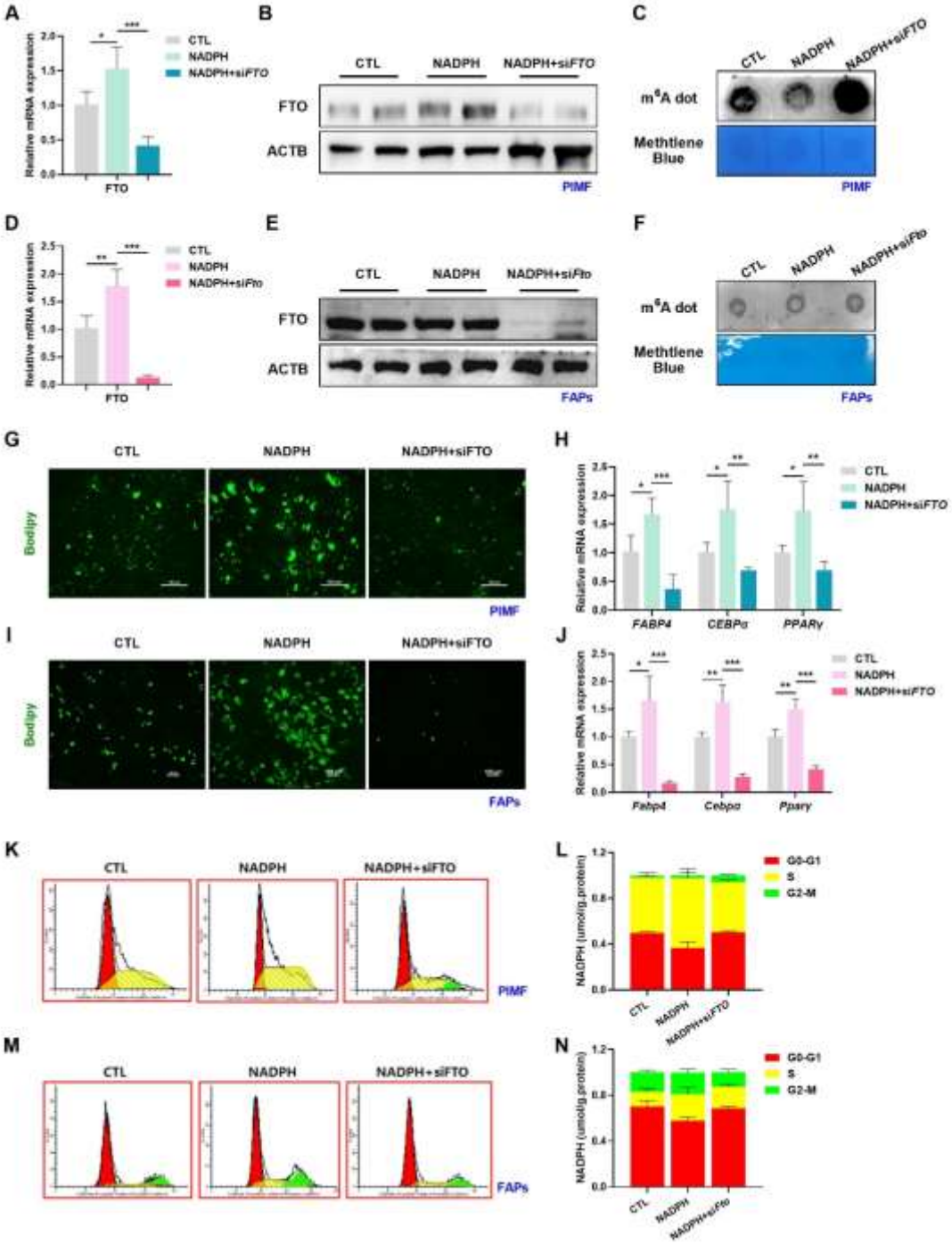

https://doi.org/10.1017/anr.2024.26 Published online by Cambridge University Press